Available online at www.sciencedirect.com
SCIENCE DIRECT®
Optics Communications 238 (2004) 105–111
OPTICS COMMUNICATIONS
www.elsevier.com/locate/optcom

Optical pulse compression in a polarization insensitive non-linear loop mirror

L. Stampoulidis [a], K. Vyrsokinos [a,*], P. Bakopoulos [a], G. Guekos [b], H. Avramopoulos [a]

[a] School of Electrical and Computer Engineering, National Technical University of Athens, 9 Iroon Polytechniou St., Zografou, GR 15773, Athens, Greece
[b] Swiss Federal Institute of Technology Zürich, ETH Hoenggerberg, CH-80923 Zürich, Switzerland

Received 19 February 2004; received in revised form 22 April 2004; accepted 28 April 2004

Abstract

We report a polarization insensitive fiber-based NOLM scheme that incorporates non-PM fibers as the non-linear medium. The circuit is configured to operate as a fiber compressor and produces narrow and pedestal-free optical pulses. The FRM stabilization ensures the excellent performance regardless of any externally applied perturbations.

PACS: 42.65.Re; 42.81.Gs; 42.87.Bg

Keywords: Non-linear optical loop mirror; Optical pulse compression; Faraday rotator mirror

1. Introduction

All-optical techniques for signal processing and conditioning are now coming of age after significant efforts during the past fifteen years. The first and arguably most heavily researched device in the all-optical domain is the non-linear optical loop mirror (NOLM) [1] and it has been extensively used to perform a diversity of functionalities [2–6]. The NOLM is a non-linear interferometer and its operation relies on the ability to impose differential phase variations due to self and cross phase modulation (SPM, XPM) in a length of fiber within the interferometer. Attractive features of these fiber-based optical devices are their good performance, ability to handle signals at very high data rates due to the ultrafast response of fiber non-linearity and simple and low cost construction. On the other hand, the use of long fiber spans as the non-linear medium makes the practical operation of fiber-based NOLMs difficult due to the intrinsic fiber birefringence, which changes temporally with physical and environmental variations. These random birefringence changes cause the state of polarization (SOP) of the two

* Corresponding author. Tel.: +30-210-7722057; fax: +30-210-7722077.
E-mail addresses: lstamp@cc.ece.ntua.gr (L. Stampoulidis), kvyrs@cc.ece.ntua.gr (K. Vyrsokinos).

0030-4018/$ - see front matter
doi:10.1016/j.optcom.2004.04.043

interfering signals to vary and result in random changes in the switching state of the NOLM [7].

A standard method to address this instability issue has been to use NOLMs constructed entirely from polarization maintaining components, including the fiber sections [8–10]. For example in [10], the authors have shown optical pulse compression utilizing a NOLM consisting of five consecutive pairs of polarization maintaining (PM) fibers with special dispersion profiles properly chosen in order to form a dispersion managed loop. However, this approach requires the availability of specialized fabrication facilities to construct PM-fibers with a strong non-linearity and a specific dispersion profile.

The realization of the faraday rotator mirror (FRM) has emerged as a reliable technique for birefringence compensation [11] and it has been used in conjunction with the self-aligned interferometer to implement simple and all-fiber arrangements for the measurement of the non-linear coefficient of various types of fibers [12,13]. In addition, the use of the FRM as a tool for optical switching applications has been investigated and has resulted in the development of linear interferometers with birefringence compensation [14,15], non-interferometric switches which rely on non-linear polarization rotation to perform demultiplexing [16] or switching [17] and non-linear, single-arm interferometers performing all-optical regeneration [18].

In the present communication, we propose a NOLM-based interferometer which is insensitive to internal fluctuations in the polarization state caused by thermal or mechanical variations (the term polarization insensitive will be used from now on). The key idea is the separation of the interferometer in two units; the interference unit, responsible for splitting and interfering of the signals and the fiber-based unit, where the non-linear phase variation takes place. To achieve stable interferometry and avoid the uncontrollable power drifts of the output signal, these two units are designed to form a polarization holding arrangement. A PM-coupler acts as the interference element, a polarization beam splitter (PBS) is used to combine and split the counter-propagating signals, whereas a FRM is arranged to compensate the polarization drifts inside the fiber section. This arrangement eliminates the requirement for an all-PM fiber structure, which is hard to assure, unless one has access to specialized fabrication facilities. The topology of the interferometer allows also for a free choice of the type of fibers incorporated inside the interferometer, facilitating the realization of various applications, from pulse compression and conditioning to demultiplexing or regeneration. As an example, we show a two-stage, NOLM pulse compressor exploiting the interplay of self phase modulation and group velocity dispersion (GVD) in non-PM, low-birefringence fibers and we experimentally verify its stability by measuring directly the polarization and power variations of the compressed signal.

2. Concept and experiment

The concept is depicted in Fig. 1, where the vertical and horizontal pulses correspond to linear polarization along the x and y axes, respectively. The orientation of the pulses represents the SOPs of the signals during their propagation in the NOLM and are included so as to describe the origin of polarization stability of the circuit. The interferometer consists of two separate parts; the PM part, which comprises a PM coupler and a polarization beam splitter (PBS), and the non-PM part, which comprises the non-PM fibers and the FRM.

The signal entering the circuit is linearly polarized along the x axis and it is split in the 50:50 PM coupler. A 90° splice is used to rotate the SOP

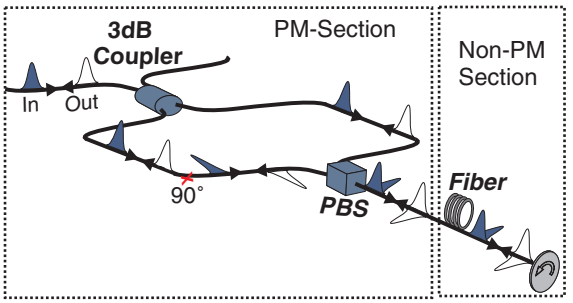

Fig. 1. Schematic diagram. The arrows represent the direction of propagation.

of the pulses traveling in the counter-clock-wise direction and the two counter-propagating signals enter a PBS through its ordinary and extraordinary axes. At the common port of the PBS the SOPs are orthogonal to each other and begin changing randomly as the two signals enter the non-PM, fiber-based stage. The incidence of the two pulse components on the FRM, causes a 90° rotation of their SOP and the reflection of the pulse components back along the same set of fibers virtually eliminates the polarization drifts within that path. Thus, all the birefringent perturbations that take place in the non-PM part of the NOLM are compensated. When the signal components arrive at the PBS the orthogonality of their SOPs is restored and rotated by 90° due to the FRM, forcing them to interchange output PBS ports and propagate through the opposite NOLM arms. The SOP of the pulses traveling in the clock-wise direction is rotated by 90° and the two linearly polarized signal components arrive at the PM coupler and successfully interfere to provide at the transmit port a signal of fixed SOP.

This technique preserves the SOP of the two interfering signals in an absolutely passive way, avoiding the use of polarization controllers and the utilization of special PM-fibers that are costly and often difficult to incorporate effectively.

The detailed experimental setup is depicted in Fig. 2. The initial pulse train was generated using a DFB laser diode at 1549.2 nm, gain switched at 2.5 GHz to provide 40 ps pulses. The pulsewidth was

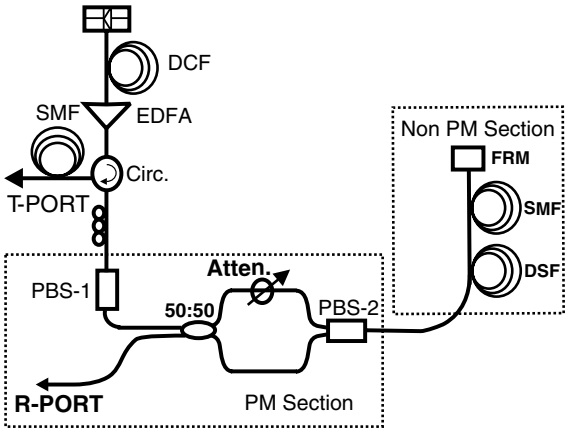

Fig. 2. Experimental setup.

reduced to 8.8 ps after linear compression in a Dispersion Compensating Fiber (DCF) with a total negative dispersion equal to −55.58 ps/nm. The resulting pulse train was amplified in a two stage EDFA consisting of a pre-amplifier and a booster amplifier, with output average power of 73 mW. A 0.6 nm filter between the two stages was used to prevent the degradation of the signal due to noise amplification at the booster amplifier.

The amplified pulses passed from port 1 to port 2 of a fiber circulator and fed into a 50:50 PM coupler through the ordinary axis of a polarization beam splitter (PBS-1), so that a linear SOP entered the NOLM. The two output ports of the PM coupler were connected to the ordinary and extraordinary axes of a second polarization beam splitter (PBS-2) and at its common port, the two counter-propagating signals appeared with orthogonal SOPs. To adjust the unbalancing of the NOLM, a polarization maintaining beam expander bearing a polarizer was used as an attenuator between one port of the PM coupler and the ordinary axis of PBS-2.

The two signals co-propagated along the nonlinear fiber medium which was 9630 m of DSF, with Dispersion of −0.44 ps/nm km at 1549.2 nm, $A_{\text{eff}} = 38\ \mu\text{m}^2$, $n_2 = 2.62 \times 10^{-20}\ \text{m}^2/\text{W}$ and used to stimulate the SPM phenomenon. The polarizer was properly rotated in order to achieve a differential phase shift of π between the two pulse components and a large frequency chirping was induced by SPM only to the signal that was not attenuated by the polarizer. The chirped pulses were successively compressed as they propagated through the dispersive medium, which was 270 m of SMF with an anomalous dispersion of 16 ps/nm km. At the FRM, the two pulse trains were reflected backwards to the SMF, where at the end of it, the first stage of the pulse compression was accomplished. The SPM phenomenon was stimulated again as the pulse trains propagated through the DSF for the second time and segregated at PBS-2. After the recombination of the two signals at the PM coupler the switched pulses were transmitted through PBS-1 and appeared at port 3 of the circulator, whereas the rejected pedestal component appeared at the reflection (R) port. At port 3 of the circulator an additional spool of 380 m of SMF was used in order to

compensate the chirp induced by the second pass through the DSF.

3. Experimental results

Fig. 3 illustrates the results recorded on a second harmonic generation (SHG) autocorrelator (upper row) and an optical spectrum analyzer (bottom row). More specifically, Fig. 3(a) shows the autocorrelation trace and the optical spectrum of the incoming pulses after the linear compression in the DCF, having a temporal and spectral width of 8.8 ps and 0.6 nm, respectively. Upon entering the DSF, the calculated energy per pulse for the attenuated signal was 2.6 pJ, whereas the corresponding value for the high power signal was 5.2 pJ. Fig. 3(b) illustrates the autocorrelation trace and the spectrum of the two signals before entering the DSF for the second time. At this point the temporal and spectral width was 4.3 ps and 0.79 nm for the attenuated signal and 3.6 ps and 1.08 nm for the high power signal. Moreover, the existence of a pedestal component is evident on the autocorrelation trace, but it can be also identified in the optical spectrum by the presence of narrow intense peaks.

A pedestal free and almost transform limited pulse was formed after the propagation through the 380 m of SMF fiber, as illustrated in Fig. 3(c). Assuming a hyperbolic secant profile, the output pulses have a temporal and spectral width of 1.85 ps and 1.44 nm, respectively. These values correspond to a time bandwidth product of 0.333 which is very close to the theoretically expected value of 0.3148. The sech shape of the transmitted pulses can also be verified by the ideal sech fit provided for both the autocorrelation trace and the optical spectrum. Both the autocorrelation trace and the optical spectrum of the pulse at T-port are also provided in logarithmic scale in Fig. 3(d) so as to examine the pedestal suppression effectiveness of the circuit. It is clear that both traces reveal the absence of the pedestal component and verify the ability of the circuit to provide high quality pulses.

In order to examine the vibration insensitivity and power clamping property of the proposed layout, we have measured the power variations of the transmitted and reflected signals for the insensitive fiber compressor and compared the results with the ones recorded for a conventional NOLM compressor assembled entirely from non-PM components. These measurements were carried out with the presence of an external vibration source which was pointed at the non-PM set of fibers. The measurements were conducted for the duration of 3 min, whereas the sampling rate was 1 sample per second.

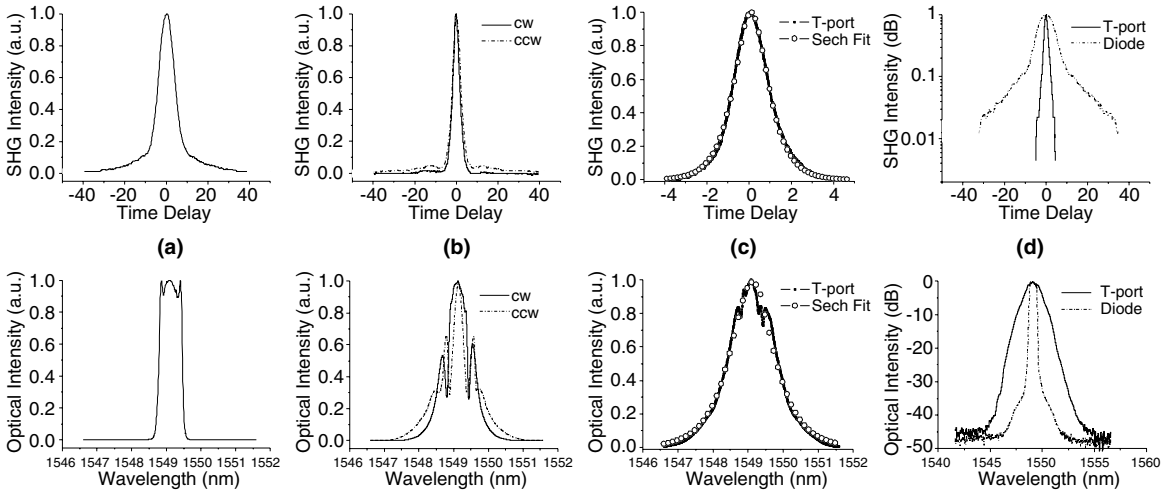

Fig. 3. Intensity autocorrelation traces (upper row) and optical spectra (bottom row) of the: (a) Input signal. (b) Signals after the 1st stage of compression (CW, clockwise; CCW, counter-clockwise). (c) Transmitted signal in linear scale and ideal sech fit. (d) Signal after DCF and transmitted signal in logarithmic scale.

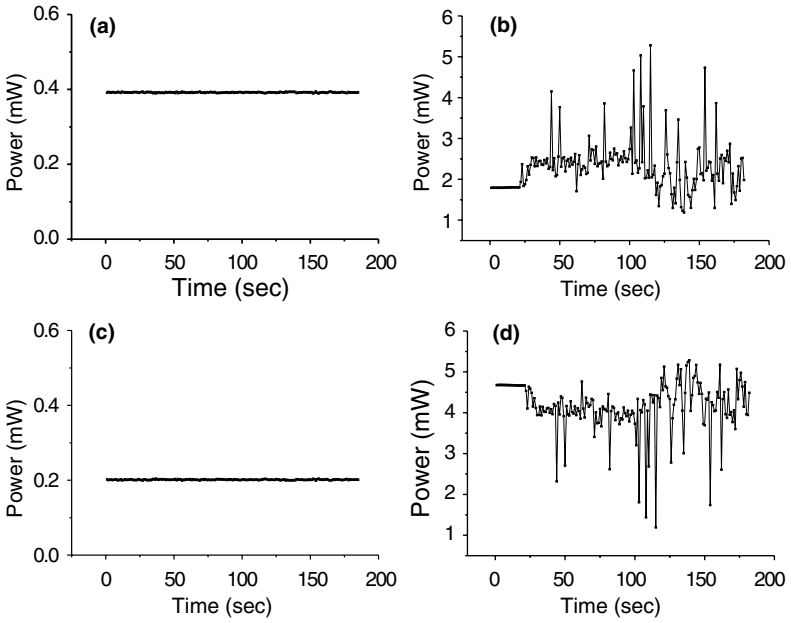

Fig. 4. Power vs. time at (a) transmit and (c) reflect port using the polarization insensitive NOLM and (b) transmit and (d) reflect port of a conventional NOLM. All the measurements were recorded in the presence of an external vibration source.

Figs. 4(a) and (b) depict the recorded transmitted power for the polarization insensitive and conventional NOLM, respectively. Fig. 4(a) shows that the power of the transmitted signal is kept almost constant regardless of any externally applied perturbations, whereas Fig. 4(b) shows that under the same conditions significant fluctuations of the transmitted power take place. It is worth mentioning that the deviation from the mean power value was in the order of 1% and 300% for the polarization insensitive circuit and the conventional NOLM, respectively. Figs. 4(c) and (d) show the same measurements for the reflected power and verify the power stability of the polarization insensitive layout and the power exchange between the two output ports of the conventional NOLM.

A polarization analyzer module was also used to test the ability of the circuit to keep the two interfering signals at the same SOP, providing a fixed polarization at its output. Figs. 5(a) and (b)

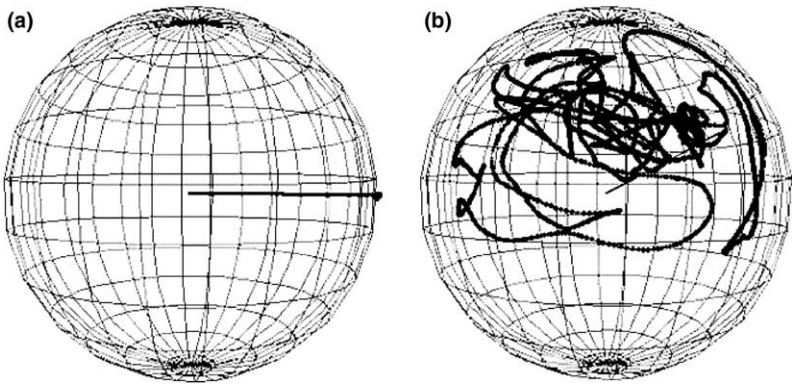

Fig. 5. Poincaré spheres at the transmit port of (a) the polarization insensitive NOLM and (b) conventional NOLM compressor.

show the evolution of the SOP of the transmitted signal pictured on the Poincaré sphere, for the polarization insensitive and the conventional NOLM compressor correspondingly. These direct polarization measurements make clear that the proposed layout was able to provide a fixed SOP at its T-port, irrespective of any birefringence perturbations, whereas the SOP of the transmitted signal in the conventional NOLM varied continuously, due to the mismatch of the SOPs of the two interfering signals. It should be noted, however, that the proposed circuit remains insensitive to the birefringence perturbations as long as they take place on time scales longer than one round-trip transit time, which in this case corresponds to about 30 μs.

4. Discussion

In the present work, we have demonstrated a technique that reduces drastically the detrimental impact of fiber birefringence on the performance of fiber-based NOLMs. The main purpose was to build a highly stable circuit avoiding the incorporation of an all PM fiber structure and for this reason a FRM was used as a birefringence compensator. To demonstrate experimentally the performance of the proposed scheme we have configured it to operate as a fiber compressor. The unbalancing of the loop was in this case performed by including attenuation in one of the arms of the PM coupler, whereas the compression took place in a set of non-PM DSF and SMF fibers. In the case of pulse compression, the ability of the circuit to passively compensate all the birefringent effects would in principle allow the incorporation of multiple compression stages generating picosecond or sub-picosecond optical pulses.

It is important to note that the topology of the circuit can be easily adjusted to realize various functionalities in the optical domain. For example, the proposed NOLM scheme can be used to implement a stable optical switch unbalanced by dispersion. In this case, an additional segment of PM fiber can be included in one of the arms of the PM coupler to induce the desired amount of dispersion, whereas the input and control signals must be suitably chosen in order to achieve a small group delay mismatch in the DSF, avoiding undesirable walk-off effects. These typical examples reveal that the operation of this polarization insensitive circuit requires no adjustments other than choosing the right set of fibers and the appropriate balancing scheme in order to implement the desired functionality.

5. Conclusion

We have presented a simple technique for stabilizing passively the performance of fiber-based NOLMs. The circuit does not require PM fibers as the non-linear medium or any polarization adjustments. The experimental verification of the polarization insensitivity of the proposed layout was made by configuring the circuit to operate as a fiber-based compressor. The power and polarization measurements showed that the power of the transmitted signal is clamped and its SOP is preserved regardless of any externally applied perturbations. The compressor produced almost transform-limited and pedestal-free pulses of 1.85 ps temporal width. In this case the inherent polarization insensitivity of the circuit allows for increased number of fiber spans in the compression stage to achieve even higher compression factors without affecting the stability of the circuit.

References

[1] N.J. Doran, D. Wood, Opt. Lett. 13 (1988) 56.
[2] K.J. Blow, N.J. Doran, B.K. Nayar, Opt. Lett. 14 (1989) 754.
[3] K. Uchiyama, T. Morioka, S. Kawanishi, H. Takara, M. Saruwatari, IEEE J. Lightwave Technol. 15 (1997) 194.
[4] N. Chi, B. Carlsson, P. Jeppesen, IEEE J. Lightwave Technol. 15 (1997) 194.
[5] M. Jinno, T. Matsumoto, IEEE J. Quantum Electron. 28 (1992) 875.
[6] L. Chusseau, E. Delevaque, Opt. Lett. 19 (1994) 734.
[7] N. Finlayson, B.K. Nayar, N.J. Doran, Opt. Lett. 17 (1992) 112.
[8] M. Jino et al., Photon. Technol. Lett. 2 (1990) 349.
[9] I. Shake, H. Takara, K. Uchiyama, S. Kawanishi, Y. Yamabayahsi, IEEE Photon. Technol. Lett. 12 (2000) 555.
[10] K.R. Tamura, M. Nakazawa, IEEE Photon. Technol. Lett. 13 (2001) 526.

[11] M. Martinelli, Opt. Commun. 72 (1989) 341.
[12] C. Vinegoni, M. Wegmuller, N. Gisin, Electron. Lett. 36 (2000) 886.
[13] C. Vinegoni, M. Wegmuller, N. Gisin, Photon. Technol. Lett. 13 (2001) 1337.
[14] A.D. Kersey, M.J. Marone, M.A. Davis, Electron. Lett. 27 (1991) 518.
[15] J. Breguet, N. Gisin, Opt. Lett. 20 (1995) 1447.
[16] T. Morioka, H. Takara, K. Mori, M. Saruwatari, Electron. Lett. 28 (1992) 521.
[17] C. Vinegoni, M. Wegmuller, B. Huttner, N. Gisin, Opt. Commun. 182 (2000) 335.
[18] J. Savage, B.S. Robinson, S.A. Hamilton, E.P. Ippen, Opt. Lett. 28 (2003) 13.